

Theoretical Studies on the Bifunctionality of Chiral Thiourea-Based Organocatalysts: Competing Routes to C–C Bond Formation

Andrea Hamza,[†] Gábor Schubert,[†] Tibor Soós,[‡] and Imre Pápai*[†]

Contribution from the Institutes of Structural Chemistry and Biomolecular Chemistry, Chemical Research Center of the Hungarian Academy of Sciences, Pusztaszeri út 59-67, H-1025 Budapest, Hungary

Received May 8, 2006; E-mail: papai@chemres.hu

Abstract: The mechanism of enantioselective Michael addition of acetylacetone to a nitroolefin catalyzed by a thiourea-based chiral bifunctional organocatalyst is investigated using density functional theory calculations. A systematic conformational analysis is presented for the catalyst, and it is shown that both substrates coordinate preferentially via bidentate hydrogen bonds. The deprotonation of the enol form of acetylacetone by the amine of the catalyst is found to occur easily, leading to an ion pair characterized by multiple H-bonds involving the thiourea unit as well. Two distinct reaction pathways are explored toward the formation of the Michael product that differ in the mode of electrophile activation. Both reaction channels are shown to be consistent with the notion of noncovalent organocatalysis in that the transition states leading to the Michael adduct are stabilized by extensive H-bonded networks. The comparison of the obtained energetics for the two pathways allows us to propose an alternative mechanistic rationale for asymmetric C–C bond forming reactions catalyzed by bifunctional thiourea derivatives. The origin of enantioselectivity in the investigated reaction is also discussed.

Introduction

Inspired by one of the key features of enzyme activity, the synergistic cooperation of a number of functional groups, synthetic chemists started to develop metal-based bifunctional Lewis base–Lewis acid catalysts for asymmetric reactions.¹ More recently, a successful metal-free concept, generally referred to as bifunctional organocatalysis, has evolved which combines H-bond donors and Lewis base functionalities in an asymmetric molecular scaffold.^{2,3} In particular, the field of bifunctional thiourea catalysis (Chart 1) is of special interest, because of the magnitude of the observed efficiencies in several fundamental enantioselective C–C bond forming reactions.^{4–8}

Despite the formidable achievements we currently witness in this field on the experimental side, our knowledge about the underlying mechanistic details is fairly limited and the role of individual active sites in the catalytic processes is not clearly established. As has been demonstrated by recent computational

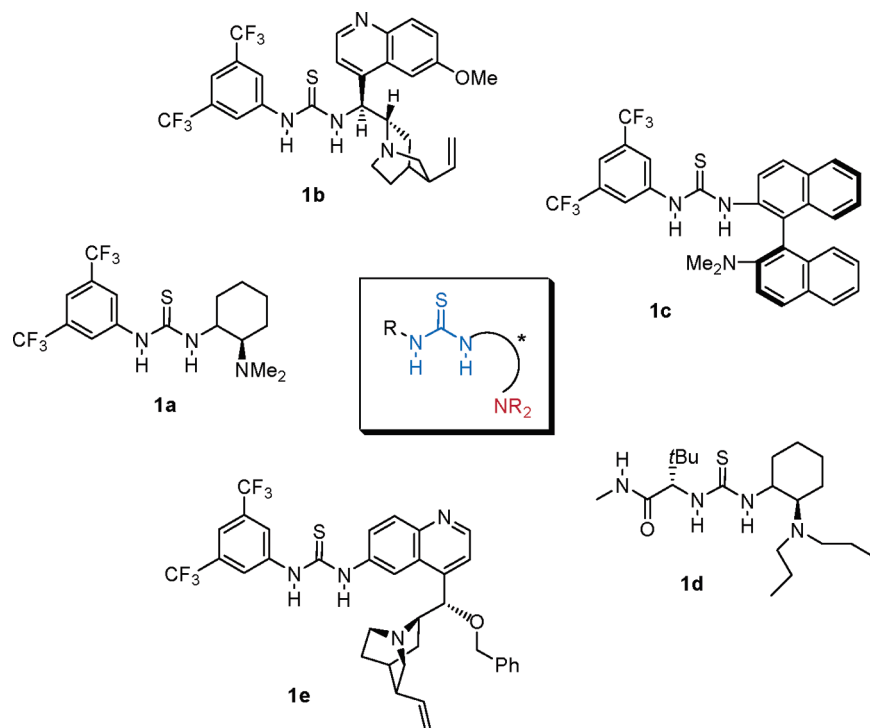
studies on proline-catalyzed asymmetric aldol reactions,⁹ accurate quantum chemical calculations can provide valuable

[†] Institute of Structural Chemistry.

[‡] Institute of Biomolecular Chemistry.

- (1) (a) Shibasaki, M.; Sasai, H.; Arai, T. *Angew. Chem., Int. Ed. Engl.* **1997**, *36*, 1236–1256. (b) Rowlands, G. *J. Tetrahedron* **2001**, *57*, 1865–1882. (c) Shibasaki, M.; Yoshikawa, N. *Chem. Rev.* **2002**, *102*, 2187–2210.
- (2) For recent general reviews on asymmetric organocatalysis, see: (a) Berkessel, H.; Gröger, H. *Asymmetric Organocatalysis*; Wiley-VCH: Weinheim, Germany, 2005. (b) Special issue on organocatalysis; Houk, K. N., List, B., Eds. *Acc. Chem. Res.* **2004**, *37*, 487–631.
- (3) For reviews discussing bifunctional organocatalysis, see: (a) Dalko, P. I.; Moisan, L. *Angew. Chem., Int. Ed.* **2004**, *43*, 5138–5175. (b) Taylor, M. S.; Jacobsen, E. N. *Angew. Chem., Int. Ed.* **2006**, *45*, 1520–1543.
- (4) For reviews concerning bifunctional thiourea-based organocatalysis, see: (a) Takemoto, Y. *Org. Biomol. Chem.* **2005**, *3*, 4299–4306. (b) Connon, S. J. *Chem.—Eur. J.* **2006**, *12*, 5418–5427.

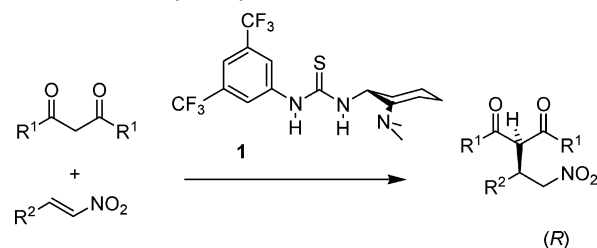
- (5) For developments and applications of cyclohexylamine-derived bifunctional thiourea catalysts, see: (a) Okino, T.; Hoashi, Y.; Takemoto, Y. *J. Am. Chem. Soc.* **2003**, *125*, 12672–12673. (b) Okino, T.; Nakamura, S.; Furukawa, T.; Takemoto, Y. *Org. Lett.* **2004**, *6*, 625–627. (c) Berkessel, A.; Cleemann, F.; Mukherjee, S.; Müller, T. N.; Lex, J. *Angew. Chem., Int. Ed.* **2005**, *44*, 807–811. (d) Berkessel, A.; Cleemann, F.; Mukherjee, S. *Angew. Chem., Int. Ed.* **2005**, *44*, 7466–7469. (e) Berkessel, A.; Mukherjee, S.; Cleemann, F.; Müller, T. N.; Lex, J. *Chem. Commun.* **2005**, 1898–1900. (f) Xu, X.; Furukawa, T.; Okino, T.; Miyabe, H.; Takemoto, Y. *Chem.—Eur. J.* **2005**, *12*, 466–476. (g) Okino, T.; Hoashi, Y.; Furukawa, T.; Xu, X.; Takemoto, Y. *J. Am. Chem. Soc.* **2005**, *127*, 119–125. (h) Fuerst, D. E.; Jacobsen, E. N. *J. Am. Chem. Soc.* **2005**, *127*, 8964–8965. (i) Dove, A. P.; Pratt, R. C.; Lohmeijer, B. G. G.; Waymouth, R. M.; Hedrick, J. L. *J. Am. Chem. Soc.* **2005**, *127*, 13798–13799. (j) Xu, X.; Yabuta, T.; Yuan, P.; Takemoto, Y. *Synlett* **2006**, *1*, 137–140. (k) Hoashi, Y.; Yabuta, T.; Yuan, P.; Miyabe, H.; Takemoto, Y. *Tetrahedron* **2006**, *62*, 365–374. (l) Steele, R. M.; Montí, C.; Gennari, C.; Piarulli, U.; Andreoli, F.; Vanthuynne, N.; Roussel, C. *Tetrahedron: Asymmetry* **2006**, *17*, 999–1006. (m) Li, H.; Wang, J.; Zu, L.; Wang, W. *Tetrahedron Lett.* **2006**, *47*, 2585–2589. (n) Li, H.; Zu, L.; Wang, J.; Wang, W. *Tetrahedron Lett.* **2006**, *47*, 3145–3148.
- (6) For developments and applications of cinchona-derived bifunctional thiourea catalysts, see: (a) McCooey, S. H.; Connon, S. J. *Angew. Chem., Int. Ed.* **2005**, *44*, 6367–6370. (b) Ye, J.; Dixon, D. J.; Hynes, P. S. *Chem. Commun.* **2005**, 4481–4483. (c) Vakulya, B.; Varga, Sz.; Csámpai, A.; Soós, T. *Org. Lett.* **2005**, *7*, 1967–1969. (d) Li, B.-J.; Jiang, L.; Liu, M.; Chen, Y.-C.; Ding, L. S.; Wu, Y. *Synlett* **2005**, 603–606. (e) Marcelli, T.; van der Haas, R. N. S.; van Maarseveen, J. H.; Hiemstra, H. *Angew. Chem., Int. Ed.* **2006**, *45*, 929–931. (f) Tillman, A. L.; Ye, J.; Dixon, D. J. *Chem. Commun.* **2006**, 1191–1193. (g) Mattson, A. E.; Zuhl, A. M.; Reynolds, T. E.; Scheidt, K. A. *J. Am. Chem. Soc.* **2006**, *128*, 4932–4933. (h) Song, J.; Wang, Y.; Deng, L. *J. Am. Chem. Soc.* **2006**, *128*, 6048–6049. (i) Bernardi, L.; Fini, F.; Herrera, R. P.; Ricci, A.; Sgarzani, V. *Tetrahedron* **2006**, *62*, 375–380.
- (7) For other types of thiourea-based bifunctional catalysts, see: (a) Herrera, R. P.; Sgarzani, V.; Bernardi, L.; Ricci, A. *Angew. Chem., Int. Ed.* **2005**, *44*, 6576–6579. (b) Wang, J.; Li, H.; Yu, X.; Zu, L.; Wang, W. *Org. Lett.* **2005**, *7*, 4293–4296. (c) Wang, J.; Li, H.; Duan, W.; Zu, L.; Wang, W. *Org. Lett.* **2005**, *7*, 4713–4716. (d) Sohtome, Y.; Takemura, N.; Iguchi, T.; Hashimoto, Y.; Nagasawa, K. *Synlett* **2006**, *1*, 144–146.

Chart 1. Representative Examples of Thiourea-Based Chiral Bifunctional Organocatalysts^a

^a References: **1a** (ref 5a), **1b** (ref 6c), **1c** (ref 7c), **1d** (ref 5h), **1e** (ref 6e).

insight into the origin of the catalysis and selectivity of organocatalytic processes, which can promote further developments. We have thus initiated theoretical investigations to elucidate the mechanism of substrate activation in reactions involving chiral thiourea catalysts. We report herein, to the best of our knowledge, the first comprehensive theoretical study aiming at exploring various mechanistic pathways in these remarkable reactions.¹⁰

Owing to their importance in synthetic chemistry, enantioselective Michael addition reactions, in particular, the addition of carbon-centered nucleophiles to nitroolefins,¹¹ represent one of the most extensively examined thiourea-catalyzed reactions.^{5a,g,6a–c,7c} Recently, a novel chiral bifunctional organocatalyst was designed by Takemoto and co-workers,^{5a} which involves an electron-withdrawing aryl substituent and a chiral tertiary amine group in thiourea. The new catalyst was shown to promote Michael reactions of various 1,3-dicarbonyl compounds with nitroolefins with excellent enantioselectivities (Scheme 1).^{5a,g} Thiourea-substituted cinchona alkaloid catalysts

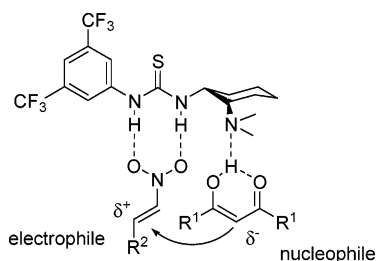
Scheme 1. Enantioselective Michael Addition of 1,3-Dicarbonyls to Nitroolefins Catalyzed by **1a**^{5g}

developed recently in several research groups have also been identified as efficient bifunctional organocatalysts in asymmetric Michael reactions,^{6a–d} and equally promising results have been obtained with novel binaphthyl-derived thiourea catalysts as well.^{7c}

According to the dual activation model proposed by Takemoto et al.,^{5g} the two substrates involved in the reaction are activated simultaneously by catalyst **1a** as shown in Scheme 2. Since nitro compounds are known to form hydrogen bonds with urea and thiourea,¹² nitroolefins have been assumed to interact with the thiourea moiety of **1a** via multiple H-bonds, enhancing in this way the electrophilic character of the reacting carbon center. On the other hand, the enolic forms of 1,3-dicarbonyls are assumed to interact with the tertiary amine group, and a subsequent deprotonation results in a highly nucleophilic enolate species. In this model, the C–C bond formation step thus takes place via the formation of a ternary H-bonded complex and the enantioselectivity of the reaction is related to the binding mode of nitroolefin to thiourea.^{5g}

- (8) For other types of bifunctional organocatalysts also known to act by means of H-bonding interactions, see: (a) Kawahara, S.; Nakano, A.; Esumi, T.; Iwabuchi, Y.; Hatakeyama, S. *Org. Lett.* **2003**, *5*, 3103–3105. (b) Matsui, K.; Takizawa, S.; Sasai, H. *J. Am. Chem. Soc.* **2005**, *127*, 3680–3681. (c) Lattanzi, A. *Org. Lett.* **2005**, *7*, 2579–2582. (d) Li, H.; Wang, B.; Deng, L. *J. Am. Chem. Soc.* **2006**, *128*, 732–733. (e) Wang, Y.; Liu, X.; Deng, L. *J. Am. Chem. Soc.* **2006**, *128*, 3928–3930.
- (9) (a) Bahmanyar, S.; Houk, K. N. *J. Am. Chem. Soc.* **2001**, *123*, 11273–11283. (b) Bahmanyar, S.; Houk, K. N.; Martin, H. J.; List, B. *J. Am. Chem. Soc.* **2003**, *125*, 2475–2479. (c) Bahmanyar, S.; Houk, K. N. *Org. Lett.* **2003**, *5*, 1249–1251. (d) Cheong, P. H.-Y.; Zhang, H.; Thayumanavan, R.; Tanaka, F.; Houk, K. N.; Barbas, C. F., III *Org. Lett.* **2006**, *8*, 811–814. (e) Rankin, K. N.; Gauld, J. W.; Boyd, R. J. *J. Phys. Chem. A* **2002**, *106*, 5155–5159. (f) Arnó, M.; Domingo, L. R. *Theor. Chem. Acc.* **2002**, *108*, 232–239.
- (10) For the first computations on thiourea-catalyzed reactions, see: (a) Schreiner, P. R.; Wittkopp, A. *Org. Lett.* **2002**, *4*, 217–220. (b) Schreiner, P. R. *Chem. Soc. Rev.* **2003**, *32*, 289–296.
- (11) Berner, O. M.; Tedeschi, L.; Enders, D. *Eur. J. Org. Chem.* **2002**, 1877–1894.

- (12) (a) Kelly, T. R.; Kim M. H. *J. Am. Chem. Soc.* **1994**, *116*, 7072–7080. (b) Linton, B. R.; Goodman M. S.; Hamilton, A. D. *Chem.–Eur. J.* **2000**, *6*, 2449–2455. (c) Bu, J.; Lillenthal, N. D.; Woods, J. E.; Nohrden, C. E.; Hoang, K. T.; Truong, D.; Smith, D. K. *J. Am. Chem. Soc.* **2005**, *127*, 6423–6429.

Scheme 2. Dual-Activation Concept Proposed by Takemoto et al.^{5g}

The primary goal of our computational study was to provide theoretical background for the above mechanistic picture, which is widely accepted in the current literature and is adopted for other types of asymmetric thiourea-catalyzed reactions as well.^{4a} The reaction we focus on in the present work is the addition of 2,4-pentadione (acetylacetonone) to *trans*- β -nitrostyrene catalyzed by **1a**, which corresponds to $R^1 = \text{Me}$ and $R^2 = \text{Ph}$ in Scheme 1. It has been shown by Takemoto et al. that this particular reaction proceeds relatively fast (within 1 h) at room temperature, affording the Michael adduct in good yield (80%) with a high enantiomeric excess (89% ee, with major (*R*) configuration).^{5g}

We have addressed several fundamental issues in the present work concerning the mechanism of the above reaction. We have first examined various conformations of the catalyst itself to see whether the orientation of the active sites is already well-defined in the free catalyst or perhaps other conformations are also feasible energetically and the organization of the active sites occurs in a later phase of the reaction. Next, we have investigated the substrate binding and the details of the process leading to the protonated form of the catalyst. In the course of identifying the intermediates and the transition states corresponding to the mechanism proposed by Takemoto et al.,^{5g} we realized that an alternative reaction pathway in the C–C bond formation process might be accessible as well. Therefore, we explored both reaction channels by locating relevant stationary points on the potential energy surface. The feasibility of the two pathways is evaluated on the basis of the obtained energetics, and the issue of enantioselectivity is also addressed in our study.

Computational Details

Two different molecular models have been considered in our work. In the simpler model, the aryl moiety of the catalyst and also the phenyl group of *trans*- β -nitrostyrene were replaced by CH_3 groups, while the other model involves the real catalyst and substrates without any simplification ($R^1 = \text{Me}$ and $R^2 = \text{Ph}$ in Scheme 1). We first searched for stationary points relevant to the investigated reaction channels using the smaller model and carried out normal coordinate analysis for the optimized structures to verify the nature of the stationary points. For each transition-state structure, we calculated the intrinsic reaction coordinate (IRC) routes in both directions toward the corresponding minima. For some of the transition states, the IRC calculations failed to reach the energy minima on the potential energy surface; therefore, in those cases we carried out geometry optimizations as a continuation of the IRC path. All these calculations were performed at the B3LYP/6-31G* level of density functional theory.¹³

The structures obtained with the simplified model were used to construct all the larger molecular models, which were again fully

optimized at the same DFT level. Since the vibrational analysis for the full system is computationally prohibited, the located energy minima and saddle points were confirmed by inspecting the eigenvalues of the Hessian at the converged structures. For the identified stationary points, we performed additional single-point energy calculations using a more extended basis set (6-311++G**) to obtain accurate energetics.

Because of the ionic nature of some of the intermediates, we found it important to evaluate the solvent effects on the relative stabilities of the identified structures. We have therefore calculated the free energies of solvation for the most important species in terms of the polarizable continuum model (PCM).¹⁴ The self-consistent reaction field (SCRFF) calculations using the PCM-UA0 solvation model¹⁵ were carried out at the B3LYP/6-31G* level for the gas-phase optimized structures. The dielectric constant in the PCM calculations was set to $\epsilon = 2.379$ to simulate toluene as the solvent medium used in the experimental study.^{5g}

It should be pointed out here that the quantitative mechanistic description of a reaction requires accurate calculations of Gibbs free energies in a solvent, which is not straightforward for the present systems for at least two reasons. In principle, the estimation of gas-phase Gibbs free energies would be possible for each intermediate and transition state because the harmonic frequencies are available with the smaller model and the zero-point energy and thermal contributions to the gas-phase energies can be estimated. However, we found that most of the structures identified as stationary points were characterized by a large number of low-frequency vibrational modes typically corresponding to collective motions of H-bonded substrates; therefore, the entropy contribution from the vibrational partition function might be significantly overestimated, causing undesirable errors in free energy calculations.¹⁶ Furthermore, although the polarizable continuum models are widely used to estimate solvation free energies of reaction components, their applicability for H-bonded systems has not been evaluated systematically. It has also been reported that, for substrate association/dissociation processes, the entropy contributions estimated for the gas phase deviate notably from the real entropic costs.¹⁷ For the above reasons, our discussion in the following section will be primarily based on gas-phase electronic energies; however, these issues will be considered again before our basic conclusions are drawn. Unless stated otherwise in the text, the relative energies reported throughout the paper are those obtained from electronic energies of gas-phase B3LYP/6-311++G** calculations.

To explore the conformational space of catalyst **1a**, constrained geometry optimizations have been carried out at the B3LYP/6-31G* level by varying systematically the dihedral angles describing the relative orientation of N–H bonds of thiourea and the rotation of the cyclohexyl moiety of **1a**. The structures corresponding to the local maxima on the potential energy curves have been used to estimate the rotational energy barriers between the stable conformation by carrying out subsequent B3LYP/6-311++G** single-point calculations for each structure.

All calculations have been carried out using the Gaussian 03 program package.¹⁸

Results and Discussion

Molecular Structure of the Catalyst. The X-ray crystallographic structure of **1a** reveals that, in the solid state, the two N–H bonds of thiourea and the amino group are oriented in the same direction.^{5g} It is generally assumed that this particular arrangement of the acidic and basic functionalities is ideal for the approach and the activation of substrates prior to the C–C

(13) (a) Becke, A. D. *J. Chem. Phys.* **1993**, *98*, 5648–5652. (b) Lee, C.; Yang, W.; Parr, R. G. *Phys. Rev. B* **1988**, *37*, 785–789. (c) Stephens, P. J.; Devlin, F. J.; Chabalowski, C. F.; Frisch, M. J. *J. Phys. Chem.* **1994**, *98*, 11623–11627.

(14) Miertus, S.; Scrocco, E.; Tomasi, J. *Chem. Phys.* **1981**, *55*, 117–129.
 (15) Barone, V.; Cossi, M.; Tomasi, J. *J. Chem. Phys.* **1997**, *107*, 3210–3221.
 (16) Ayala, P. Y.; Schlegel, H. B. *J. Chem. Phys.* **1998**, *108*, 2314–2325.
 (17) See, for example: (a) Cooper, J.; Ziegler, T. *Inorg. Chem.* **2002**, *41*, 6614–6622. (b) Tobisch, S. *J. Am. Chem. Soc.* **2005**, *127*, 11979–11988.
 (18) Frisch, M. J.; et al. *Gaussian 03*, revision C.02; Gaussian, Inc.: Wallingford, CT, 2004.

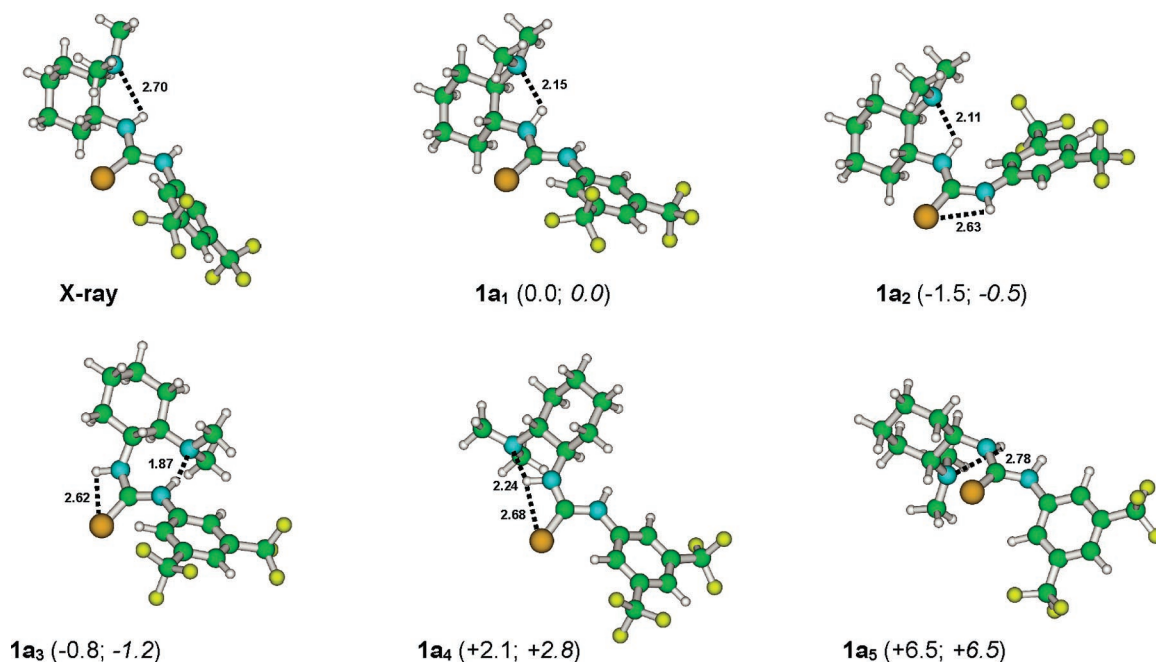


Figure 1. X-ray structure of catalyst **1a** and the conformers identified as energy minima. Bond distances of stabilizing H-bonds are given in angstroms, and relative stabilities (kcal/mol) with respect to **1a₁** are shown in parentheses (PCM-corrected values are shown in italics).

coupling process. The importance of appropriate orientation of active catalytic sites has recently been demonstrated for cinchona-derived organocatalysts.^{6a,c} To provide information on prevailing conformations of catalyst **1a** in solution, we carried out a detailed conformational analysis and identified several stable structures on the conformational landscape, which are depicted in Figure 1.

Isomer **1a₁**, which corresponds to the X-ray structure, is characterized by an intramolecular N–H···N hydrogen bond formed between the tertiary amine and the neighboring N–H group. The calculated N···H bond distance in **1a₁** ($R_{N···H} = 2.15$ Å) is much shorter than the value observed in the solid state ($R_{N···H} = 2.70$ Å), wherein intermolecular hydrogen-bonding interactions between thiourea units are known to exist,^{5c,s} and their presence certainly weakens the intramolecular N–H···N hydrogen bond.¹⁹ Structure **1a₁** is indeed predicted to be one of the most stable conformations; however, the calculations show that several other structures may have similar stabilities (see Figure 1). For instance, isomer **1a₂**, derived by a rotation along the C–N(aryl) bond of thiourea, is predicted to be 1.5 kcal/mol more stable than **1a₁**, which can be attributed to a weak N–H···S-type interaction observed in **1a₂**. The amine group can also interact with the distant N–H bond, and because of enhanced acidity of this N–H group, a relatively strong H-bond is formed ($R_{N···H} = 1.87$ Å), leading to a conformation (**1a₃**) that is slightly more stable than **1a₁**. The stabilizing N–H···N and N–H···S interactions are weaker in **1a₄**, because the same N–H proton interacts with two basic centers, so **1a₄** becomes slightly less favored energetically. In structure **1a₅**, only the relative orientation of the cyclohexyl moiety differs from that in **1a₁**, also giving rise to an internal N–H···N bond; however, **1a₅** is predicted to be 6.5 kcal/mol above **1a₁**. We note that the stability order in the **1a₁**–**1a₅** series of isomers remains

essentially unchanged if solvent effects are included in the estimation of relative energies, except that isomer **1a₃** becomes the energetically most favored structure with the inclusion of solvation energies (see Figure 1).

Assuming that the entropy contributions to the free energies of the presented structures are similar, and also that the presence of aprotic solvent molecules does not notably alter the relative stabilities of these conformers, we may conclude that, in solution, the structure of catalyst **1a** does not necessarily correspond to that observed in the solid state, but other energetically preferred conformations are populated as well. These structures are likely in a dynamic equilibrium in solution, since our calculations indicate that some of the low-lying conformations of **1a** can easily interconvert at room temperature. For example, the energy barriers related to the **1a₁** → **1a₂** and **1a₃** → **1a₄** transitions estimated from the conformational analysis are rather low (5.4 and 6.5 kcal/mol), whereas the gap between **1a₁** and **1a₃** is found to be moderate (12.8 kcal/mol) (for the details of conformational analysis, see the Supporting Information).

Substrate Binding and Catalyst Protonation. In view of the above results pointing to a certain degree of conformational flexibility of catalyst **1a** in solution, an obvious question arises about possible effects that may organize the active centers to their optimal arrangement. Substrate binding can certainly influence the conformational distribution, as both substrates are expected to favor double H-bond coordination, which can only be achieved preferentially with **1a₁**. Indeed, we find that the most stable forms of the adducts formed via the interaction of *trans*- β -nitrostyrene and the enolic form of acetylacetone²⁰ with catalyst **1a** correspond to bidentate coordination modes as shown in Figure 2.²¹ Hereafter, these two substrates will be denoted

(19) The discrepancy between the computed and X-ray $R_{N···H}$ values may partially arise from the fact that the positions of the H atoms in the X-ray measurements are not determined as such, but they are rather estimated by a fitting procedure using a simple model.

(20) The keto–enol tautomeric equilibrium of acetylacetone is known to be shifted toward the enolic form due to internal hydrogen bonding; see, for example: Moriyasu, M.; Kato, A.; Hashimoto, Y. *J. Chem. Soc., Perkin Trans. 2* **1986**, 515–520.

(21) Several other coordination modes have been located as local minima for both binary complexes, which are reported in the Supporting Information.

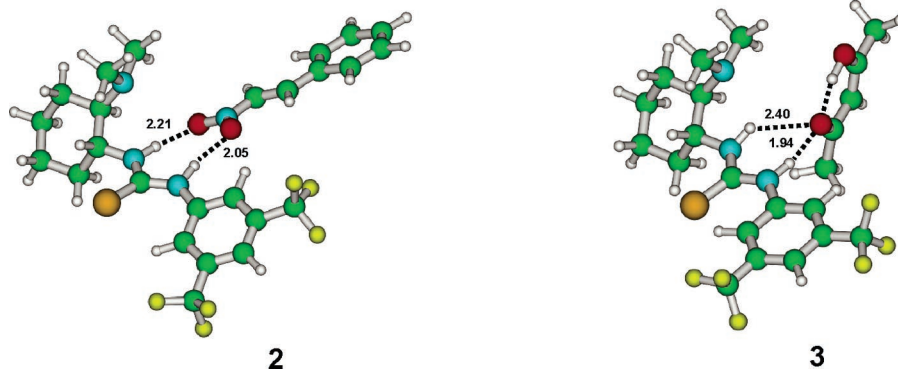


Figure 2. Optimized structures of the most stable catalyst–substrate adducts. Bond distances characteristic for H-bonds are given in angstroms.

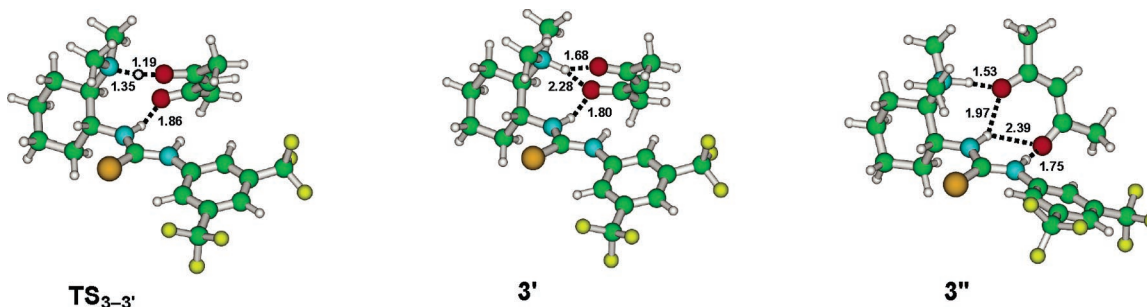


Figure 3. Optimized structures of stationary points located for the protonation process between catalyst **1a** and **NuH**.

as **EI** (*trans*- β -nitrostyrene) and **NuH** (acetylacetonone), which refer to their electrophile/nucleophile character in the reaction (see Scheme 2).

In complex **2**, the substrate forms a bidentate H-bond with **1a₁** in a nearly coplanar arrangement with the thiourea unit, and the calculated substrate binding energy is 7.6 kcal/mol. For comparison, the binding energy in a monodentate complex formed between **1a₂** and **EI** is 5.7 kcal/mol, which clearly illustrates the effect of substrate binding on the conformational distribution of the catalyst, as the stability order between the **1a₁** and **1a₂** configurations is interchanged upon the coordination of **EI**. The association between substrate **NuH** and **1a** is characterized by a bifurcated H-bond formed between the carbonyl moiety of **NuH** and the N–H groups; however, the molecular plane of the coordinated enol is perpendicular to thiourea (see Figure 2). Due to the difference in the acidity of the two N–H groups in **1a**, the N–H \cdots O bonds adjacent to the aryl substituent are clearly stronger in both adducts. The binding energy of **NuH** in complex **3** is predicted to be 7.3 kcal/mol, which is rather similar to that of **EI** in complex **2**, implying that no preference can be established for the formation of the two types of adducts in the reaction.

Despite the bidentate nature of the hydrogen bonds in **2** and **3**, the catalyst–substrate interactions can be classified into the weak, or at most moderate, category according to the calculated association energies.^{3b} Moreover, these binary complexes cannot be regarded as well-defined rigid structures because of their flexibility related to low-energy collective motions (hindered translations and rotations) with respect to the catalyst. Our test calculations carried out with the same computational approach for selected H-bonded systems with available experimental thermochemical data suggest that the free enthalpy change related to the **1a** + **EI** \rightarrow **2** and **1a** + **NuH** \rightarrow **3** association processes in solution are very likely endergonic ($\Delta G > 0$) (see

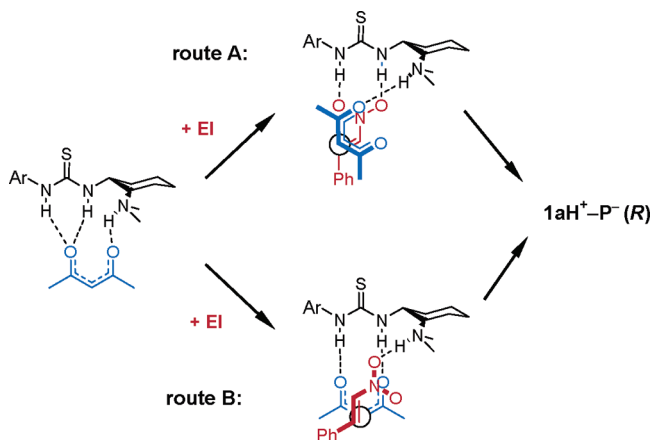
the Supporting Information), because the entropic effects of both complexations exceed the binding exothermicities.²² It is therefore anticipated that the relative concentration of the binary catalyst–substrate adducts in the reaction mixture is probably rather low; therefore, these species might not be easily detected spectroscopically at normal conditions.

Furthermore, we find that a proton transfer from the coordinated enol to the amine group of the catalyst can easily take place, as the transition state related to this process (**TS_{3-3'}**) represents a relatively small energy barrier (6.6 kcal/mol) with respect to adduct **3** (see Figure 3) and the resulting ion pair (**3'**) is predicted to be only 2.2 kcal/mol above **3**. The enolate ion in **3'** is stabilized via multiple N–H \cdots O bonds that involve the cationic amine moiety and one of the N–H groups of thiourea as well. Another form of the ion pair (**3''**), also characterized by multiple N–H \cdots O hydrogen bonds, has been identified in our calculations, which is predicted to be 2.0 kcal/mol less stable than structure **3'**. In complex **3''**, the enolate is tilted from its original position so that the number of N–H \cdots O bonds is maximized because all three N–H units become involved in the H-bonded network.

Due to the ionic nature of species **3'** and **3''**, the energetics of the protonation process is found to be more favorable if solvent effects are considered. For instance, the formation of the multiply bonded ion pair **3''** becomes permitted energetically, and the energy difference between **3'** and **3** also decreases. The relative energies of **3'** and **3''** in the solvated model are 0.7 and -0.5 kcal/mol as compared to the energy of structure **3**. We also mention that, at this level of theory, the energy barriers corresponding to the **3** \rightarrow **3'** protonation and **3'** \rightarrow **3''** rearrangement are 5.8 and 0.9 kcal/mol, respectively. These results indicate that the protonation of the catalyst at the amino group

(22) Wittkopp, A.; Schreiner, P. R. *Chem.–Eur. J.* **2003**, *9*, 407–414.

Scheme 3. Two Reaction Routes Envisioned for the Michael Addition of Acetylacetone to Nitrostyrene^a



^a Note that both pathways lead to the formation of the (*R*) configuration of the Michael adduct in the present arrangement of the substrates. Notation: **EI** = nitroolefin, **1aH⁺** = protonated catalyst, Ar = 3,5-(bis(trifluoromethyl)phenyl), **P⁻** = nitronate Michael adduct.

is a both kinetically and thermodynamically feasible process in the present catalytic reaction, which is in line with the model suggested by Takemoto et al. for Michael reactions of malonates.^{5g} We mention that the ion pair mechanism is thought to operate in a number of reactions catalyzed by quaternary ammonium ions and amines in heterogeneous phases.²³

As seen in Figure 3, the N–H groups of thiourea have an important role in the protonation process, because they provide a binding site for the nucleophile species in the near proximity of the tertiary amine (see complex **3**) and also stabilize the catalyst–enolate ion pair via multiple hydrogen bonds. It appears reasonable to assume that the formation of the ion pair (**3'** and **3''**), which presumably occurs prior to nitroolefin activation, is another organizing effect concerning the availability of the asymmetric binding pocket for the reacting substrates. Our calculations attempting to describe the protonation of the catalyst in the presence of H-bonded nitroolefin failed to locate an encounter complex for the approach of **NuH** to the amine group, providing additional support for the above sequence of substrate activation.

Two Reaction Pathways for C–C Bond Formation. Two distinct reaction pathways can be envisioned for the C–C bond formation step of the catalytic process (see Scheme 3). According to the mechanism proposed by Takemoto et al.,^{5g} the nitroolefin interacts with the thiourea moiety of complex **3'**, forming a ternary complex, wherein both substrates are activated so the C–C bond formation can occur to produce the nitronate adduct (**1aH⁺–P⁻(R)** in Scheme 3). Alternatively, the facile **3' → 3''** rearrangement may allow the interaction of nitroolefin with the cationic N–H group of the protonated amine, resulting in a ternary complex which can also be considered as a precursor for the C–C coupling step. In what follows in this section, we

describe the structures and energetics of the stationary points located on the potential energy surface along the two reaction channels.

The structures corresponding to the coordination of nitroolefin to thiourea and subsequent C–C bond formation (route A) are presented in Figure 4. The optimized geometry of the ternary complex **4** identified on this route is consistent with the picture that a nitro compound can bind to complex **3'** via double H-bonds while the enolate is still attached to the catalyst in a coplanar manner with nitroolefin. The binding energy of **EI** in the ternary complex is found to be quite small, since complex **4** lies only 1.6 kcal/mol below the **3' + EI** dissociation asymptote. The small energy stabilization is related to the absence of enolate–thiourea H-bonding interactions in the binary ion pair (**3'** or **3''**), which is only partially compensated by the strengthening of H-bonding interactions between thiourea and **EI** as compared to those in complex **3** (see H···O distances in **3** and **4**).

Nevertheless, the C–C bond formation between the nucleophilic center of the enolate anion and the electron-deficient prochiral carbon of nitrostyrene can take place via transition-state **TS_{4–5}**, which represents a moderate energy barrier (11.6 kcal/mol) for the coupling process.²⁴ The structure of **TS_{4–5}** indicates that the formation of the C–C bond is coupled with the weakening of the catalyst–enolate interaction, which is due to charge transfer occurring from the anionic enolate to nitroolefin. Also as a result of negative charge delocalization, the H-bonded linkage between the nitro group and thiourea is strengthened. These effects become so significant on the product side of the C–C coupling step that the formed nitronate adduct is bound only with its nitro group to the catalyst via multiple N–H···O bonds. The calculations predict structure **5** to be 1.0 kcal/mol more stable than ternary complex **4**.

The deprotonation of the catalyst to yield the *aci* form of the Michael adduct followed by a dissociation step and *aci*-nitro tautomerization is a likely process in the remaining part of the reaction pathways; however, the investigation of these steps was out of the scope of our present work.

The structures of the intermediates and the associated transition state located on the alternative reaction channel (route B) are shown in Figure 5. Interestingly, we find that ternary complex **6** is notably more stable than the one located on route A, as **6** lies 2.9 kcal/mol below **4** (4.5 kcal/mol below the **3' + EI** limit). In complex **6**, the enolate is stabilized by multiple H-bonds similar to that in **3''**, and substrate **EI** binds to the protonated amine group of the catalyst. The relatively short H···O distances found for the CH₃···O₂N contacts suggests that, in addition to the N–H···O hydrogen bond, attractive C–H···O₂N-type interactions may also contribute to the stabilization of the trialkylammonium···nitroolefin bonding. The magnitudes of stabilizing N⁺–CH₃···O=C interactions have recently been evaluated, and their role in stereoselective catalysis has also been discussed.²⁵ For instance, the mechanistic model of contact ion-pairing proposed by Corey et al. for asymmetric phase-transfer alkylation reactions^{23a} assumes electrostatic interactions between the electrophile and the cationic tetraalkylammonium unit of the catalyst in Michael reactions.^{23d}

(23) For reactions catalyzed by quaternary ammonium salts of cinchona alkaloids, see: (a) Corey, E. J.; Xu, F.; Noe, M. C. *J. Am. Chem. Soc.* **1997**, *119*, 12414–12415. (b) Corey, E. J.; Bo, Y.; Busch-Petersen, J. *J. Am. Chem. Soc.* **1998**, *120*, 13000–13001. (c) Corey, E. J.; Zhang, F.-Y. *Org. Lett.* **1999**, *1*, 1287–1290. (d) Zhang, F.-Y.; Corey, E. J. *Org. Lett.* **2000**, *2*, 1097–1100. For applications in heterogeneous amine catalysis, see: (e) Bass, J. D.; Solovoyov, A.; Pascall, A. J.; Katz, A. *J. Am. Chem. Soc.* **2006**, *128*, 3737–3747. (f) Diezi, S.; Ferri, D.; Vargas, A.; Mallat, T.; Baiker, A. *J. Am. Chem. Soc.* **2006**, *128*, 4048–4057.

(24) For comparison, energy barriers estimated for the C–C bond formation step in proline-catalyzed intermolecular aldol reactions range between 9 and 15 kcal/mol; see ref 9e,f.

(25) Cannizzaro, C. E.; Houk, K. N. *J. Am. Chem. Soc.* **2002**, *124*, 7163–7169.

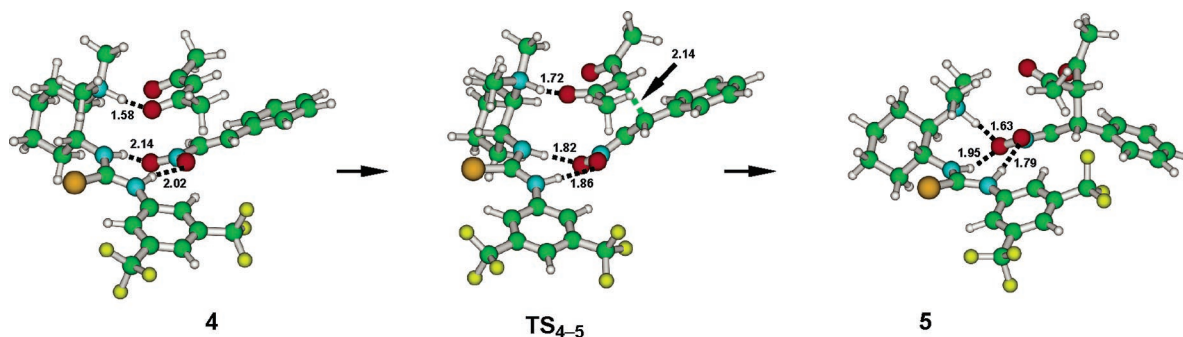


Figure 4. Optimized structures and selected geometric parameters of the stationary points located on route A.

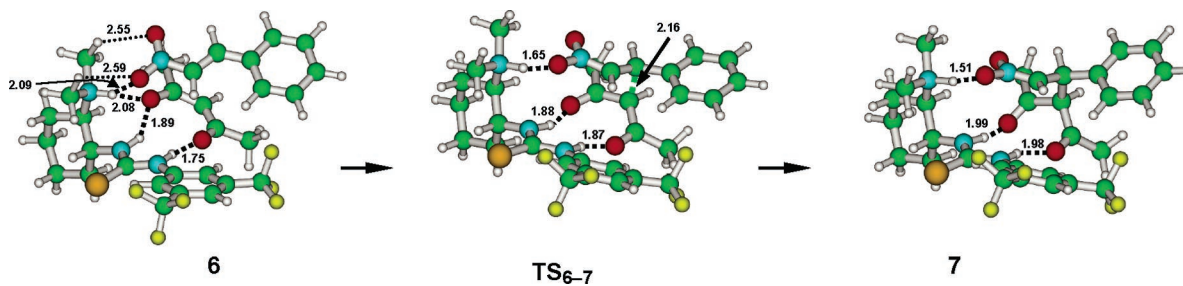


Figure 5. Optimized structures and selected geometric parameters of the stationary points located on route B.

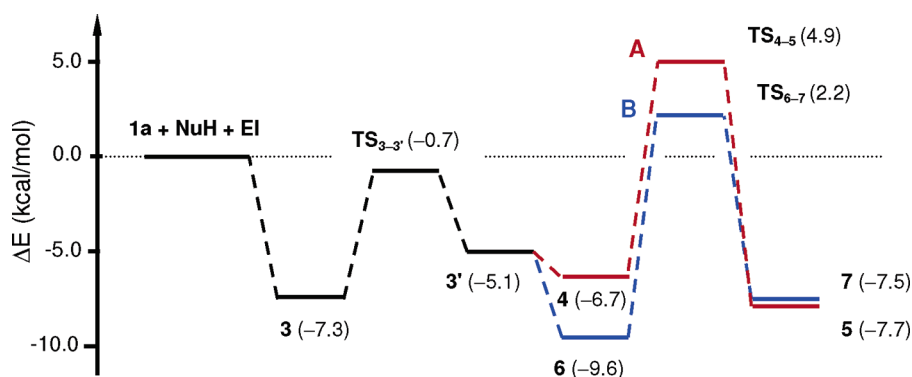


Figure 6. Energy profile of the C–C bond formation pathways corresponding to the formation of the (*R*) configuration of products as obtained from gas-phase calculations.

On route B, the C–C bond formation is predicted to be a kinetically feasible process as well which proceeds via transition-state TS_{6-7} lying 11.8 kcal/mol above the corresponding ternary complex **6**. This process is also accompanied by structural changes characteristic for intermolecular charge transfer between the reacting substrates. The N–H \cdots O $_2$ N interaction becomes apparently stronger in TS_{6-7} , whereas the enolate carbonyl is displaced from the vicinity of the protonated amine and is bound only to thiourea via bidentate N–H \cdots O bonds.

Additional weakening of these latter bonds is encountered in complex **7**, and the protonation of the nitronate adduct by a proton transfer from the amine group may further facilitate the dissociation of the product molecule from the catalytic pocket. In the gas-phase model, the calculations predict that complex **7** is 2.1 kcal/mol above the ternary complex; however, this energy difference decreases to 0.3 kcal/mol if solvent effects are taken into account in the calculations.

Overall Energetics: Comparison of Two routes. To parallel the energetics of the two C–C coupling reaction channels, we first examine the gas-phase relative energies of the elementary steps discussed above. The energy profile derived from the

B3LYP/6-311++G** electronic energies of the most relevant species identified in our study is plotted in Figure 6.

It is apparent from the diagram that the energy barrier of the $3 \rightarrow 3'$ protonation step is clearly lower than those obtained for the two possible coupling processes, which means that the C–C bond formation can be regarded as the rate-determining step for the investigated section of the reaction. As all the elementary steps prior to C–C coupling (substrate binding, protonation) are found to be kinetically mobile and thermodynamically reversible, the various forms of binary and ternary complexes are in thermodynamic equilibrium. Consequently, the relative probability of C–C bond formation along the two reaction channels (routes A and B) is related to the relative energies of the two transition states. Since TS_{6-7} is predicted to lie 2.7 kcal/mol lower in energy than TS_{4-5} , the gas-phase model predicts that the C–C bond formation in the present Michael addition reaction occurs predominantly on route B.²⁶ A similar conclusion can be drawn from the energetics that incorporate solvent effects via the polarizable continuum model because the calculated

(26) Using absolute rate theory, the ratio of the reaction rates on the two pathways is $v_A:v_B = 1:100$ ($\ln(v_A/v_B) = -\Delta E(\text{TS}_{4-5} - \text{TS}_{6-7})/RT$, with $-\Delta E(\text{TS}_{4-5} - \text{TS}_{6-7}) = 2.7$ kcal/mol and $RT = 0.59$ kcal/mol).

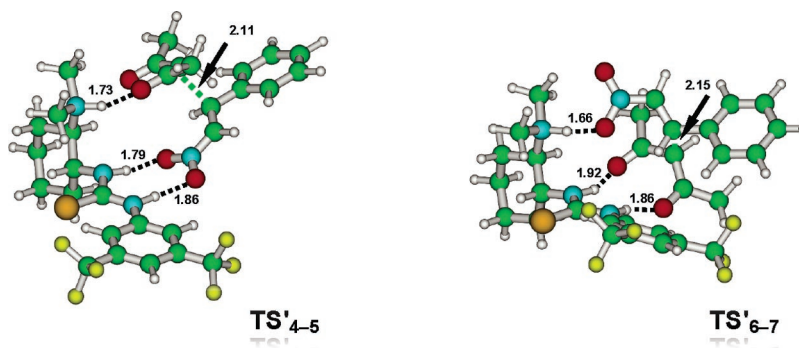


Figure 7. Optimized structures and selected geometric parameters of transition states yielding the (*S*) product.

energy difference between the two transition states is 1.9 kcal/mol if the solvation energies are taken into account.²⁷

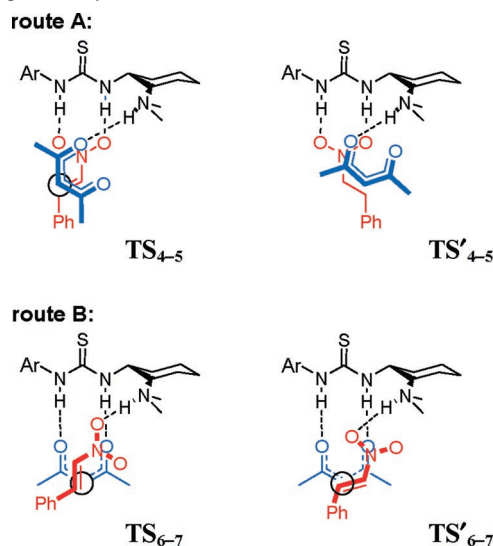
As noted before, the prediction of accurate Gibbs free energy profiles for reactions taking place in solutions remains a challenge for present-day quantum chemical methods. The absolute errors might be significant, particularly for association/dissociation steps; however, for isomeric processes, such as the two C–C bond formation routes in our case, favorable error cancellation is expected, leading to smaller relative errors as compared to their absolute values. We have thus estimated the gas-phase Gibbs free energies of **TS**_{4–5} and **TS**_{6–7} by using the zero-point energy and thermal corrections (for *T* = 298 K) obtained for the simplified molecular models and found that the transition state on route B is favored by 1.6 kcal/mol, showing the same stability order for the two reaction channels as found above.

All these results suggest that, for the present reaction, route B represents an energetically preferred pathway for the C–C coupling process as compared to route A. It is notable that the formation of ternary complex **6** on route B is also compatible with the results of a kinetic study reported by Takemoto and co-workers which indicates that the reaction is first-order in both substrates and catalyst.^{5g}

Enantioselectivity. Another intriguing aspect to be explored for the investigated reaction is the origin of enantioselectivity, which is certainly controlled in the C–C bond formation step, as the absolute configuration of the Michael adduct is determined by the attacking face of substrate **EI** approaching the H-bonded enolate of the ion pair. All our results presented thus far refer to pathways leading to the (*R*) configuration of the product. Here, we present the structural and energetic characteristics of the C–C coupling step for the formation of the (*S*) enantiomeric form.

Because the electron density distributions on the two oxygens of nitroolefin are practically identical (as judged from the calculated net atomic Mulliken charges), and the phenyl end of **EI** is not in direct contact with the catalyst, the ternary complexes identified on routes A and B toward the (*S*) product lie very close in energy (to within 0.5 kcal/mol) to their (*R*) counterparts **4** and **6** (for isomeric structures, see the Supporting Information). However, the energy barriers represented by **TS'**_{4–5} and **TS'**_{6–7} (see Figure 7), which lead to the (*S*) product, are predicted to be notably higher on both routes. The calculations show that, on route A, **TS'**_{4–5} is 2.6 kcal/mol less favored than **TS**_{4–5}, whereas on the alternative route, transition-state

Scheme 4. Schematic View of Transition States Leading to (*R*) and (*S*) Isomers of Michael Products on Two Alternative C–C Coupling Pathways

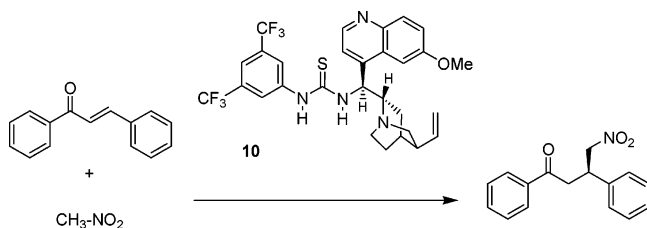


TS'_{6–7} is found to be 2.4 kcal/mol less stable than **TS**_{6–7}. These energy differences correspond to high enantioselectivities for both reaction routes (98% ee and 97% ee for routes A and B) which are in qualitative agreement with the experimental findings (89% ee).^{5g} Because of the similarity of the calculated ee values, these results do not provide any additional information regarding the feasibility of the two competing C–C coupling reaction channels.

Close inspection of the four transition states reveals very similar N–H···O bond distances in structures belonging to the same route (A or B), indicating that the H-bonding environment provided by the three N–H groups of the ion pair has a key role in the stabilization of transition states and the evolving products. There are, however, substantial differences in the relative orientations of the reacting components upon the formation of the two enantiomeric species, which is valid for both reaction channels A and B. In transition states affording the (*R*) product (**TS**_{4–5} and **TS**_{6–7}), the substrates are aligned in a staggered conformation along the forming C–C bonds to minimize steric intermolecular interactions (see Scheme 4). These favorable orientations cannot be adopted in **TS'**_{4–5} and **TS'**_{6–7} because the electrophilic carbon center of **EI** is displaced from its ideal position when the attacking face of **EI** is switched and the C–C bond formation can only take place with a compromise of either the H-bonding catalyst–substrate interactions or the staggered geometry of the reacting molecules. The

(27) For the full-energy diagram obtained with the solvated model, see the Supporting Information.

Scheme 5. Enantioselective Michael Addition of Nitromethane to *trans*-Chalcone Catalyzed by a Bifunctional Cinchona Organocatalyst^{6c}



optimized structures of **TS'**₄₋₅ and **TS'**₆₋₇ indicate that the C–C bonds of the two substrates are nearly eclipsed and therefore destabilize both transition states. These results underline the importance of the relative geometric arrangement of the acidic and basic groups in a bifunctional catalyst, which should be compatible predominantly with the transition state of the desired stereoisomer to achieve acceptable stereoselection.

Mechanistic Proposal and Its Application to an Analogue Cinchona System. Our analysis of the two C–C bond formation pathways for the present reaction, in particular the preference of route B in terms of the activation barrier, leads us to postulate an alternative mechanism for enantioselective Michael addition reactions catalyzed by recently developed thiourea-based bifunctional catalysts. The new mechanism emerging from our theoretical study is consistent with the notion of dual activation suggested previously, since the catalyst serves to activate both substrates simultaneously in a ternary complex. However, the new feature in our proposal is that the activation of the

electrophile component is achieved through the interaction with the protonated amino group of the catalyst rather than with the H-bond donors of thiourea. The key intermediate in this model is the catalyst–nucleophile ion pair, which is characterized by multiple H-bonds involving the N–H groups of thiourea as well. The thiourea's acidic functionalities along with the N–H bond of the protonated amine play an important role in the stabilization of the transition states leading to the major isomer of the Michael adduct, because they form a well-defined chiral environment that induces stereoselectivity in the reaction.

To gauge the generality of this mechanistic scenario, we have initiated a theoretical investigation on another catalytic system, namely, the conjugate addition of nitromethane (**8**) to *trans*-chalcone (**9**) catalyzed by a thiourea-substituted cinchona derivative (**10**) (Scheme 5). This reaction was also shown to perform remarkably well in terms of enantioselectivity even at higher temperature.^{6c} The nitroalkane acts as a nucleophile in related catalytic addition reactions;^{5b,f} thus, the formation of a protonated catalyst–nitronate intermediate is expected in the present reaction as well.

Our DFT calculations carried out at the same level as in the rest of the paper reveal a close resemblance between the structures of the identified catalyst–nitronate ion pair and complex **3''**, as the former binary complex is also stabilized by multiple N–H···O bonds involving the three acidic sites of the protonated catalyst (see structure **11** in Figure 8).

The two types of ternary complexes leading to the major enantiomeric form (*R*) of the nitromethane adduct on the alternative C–C coupling channels are also depicted in this figure. We find that complex **12**, which corresponds to the

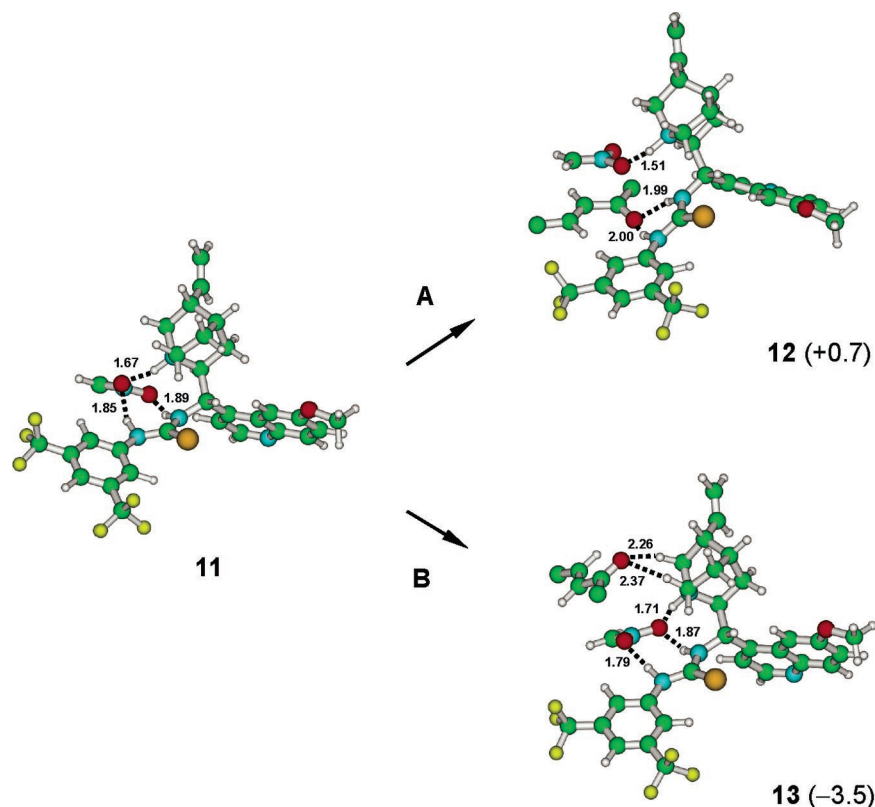


Figure 8. Optimized structures and selected geometric parameters of the ion pair and the two types of ternary complexes corresponding to routes A and B in asymmetric Michael addition of nitromethane to *trans*-chalcone (the phenyl groups of *trans*-chalcone are omitted for clarity). Binding energies relative to **11** + chalcone are given in parentheses (kcal/mol).

coordination of the electrophilic species to thiourea, is 4.2 kcal/mol less stable than the ternary complex formed on route B, indicating that the disruption of the intermolecular H-bonded network in the ion pair, which is unavoidable on route A, is energetically unfavored. On the other hand, the binding of the keto compound can preferentially take place through the interaction with the trialkylammonium group while keeping the multiple H-bonded structure of the ion pair.²⁸

These results provide further support for the new mechanistic proposal that the electrophilic substrate in asymmetric Michael addition reactions can also be activated by the protonated amine group of a bifunctional organocatalyst prior to C–C bond formation.

Concluding Remarks

We have presented a detailed computational mechanistic study of a reaction belonging to the family of asymmetric Michael addition reactions promoted by bifunctional noncovalent catalysts. The main conclusions of our work, which may extend our understanding of the bifunctionality of recently designed thiourea-based organocatalysts and perhaps assist in further conceptual developments, can be summarized as follows.

(1) Catalyst **1a** cannot be regarded as a conformationally rigid molecule in solution having the active acidic and basic functionalities oriented in the same direction as found in the solid state, because other low-lying conformations are easily accessible on the potential energy surface.

(2) Substrate binding occurring preferentially via bidentate H-bonds can induce a certain degree of structural organization. However, the optimal structural arrangement of the active sites is ultimately attained via the protonation of the catalyst's basic center by the nucleophilic substrate, because the resulting ion pair adopts a multiply H-bonded structure. We found the protonation process to be kinetically allowed and reversible.

(3) The generally accepted mechanism for adduct formation in relevant catalytic Michael addition reactions involves electrophile activation through substrate binding to thiourea, yielding a ternary complex, and subsequent C–C bond formation between simultaneously activated components. Our calculations

underline that this pathway is feasible both kinetically and thermodynamically.

(4) We have described an alternative reaction mechanism for the C–C coupling steps which corresponds to electrophile activation by the protonated amine group of **1a** without breaking the multiple N–H···O bonds in the ion pair. The ternary complex and the related transition state along this route have been shown to be notably more stable than those on the other pathway.

(5) Both reaction pathways account for the observed enantioselectivity. This property is governed by the shape of the H-bonded network provided by the three acidic N–H groups of the protonated catalyst, which determines the preferential relative orientation of the approaching substrates and therefore induces stereoselectivity.

(6) We anticipate that the alternative mechanism described for the present Michael addition reactions may also be operative in other types of asymmetric thiourea-catalyzed C–C bond forming organic transformations that involve nucleophiles capable of undergoing base activation and electrophiles with strongly polarized carbonyl or nitro functionalities. In our first attempt to explore the general validity of the proposed mechanism, we identified two types of ternary complexes in another thiourea-catalyzed system and found similar trends for their relative stabilities.

Further mechanistic studies are certainly required to assess the generality of the proposed mechanism and also to identify the factors that govern the relative energetics of the two alternative C–C coupling reaction pathways. Work along these lines is in progress in our group.

Acknowledgment. This work has been supported by the Hungarian Research Foundation (OTKA, Grant K-60549). Computer facilities provided by the NIIF Supercomputer Center in Budapest are greatly acknowledged.

Supporting Information Available: Cartesian coordinates and absolute energies of all stationary points located on the potential energy surface, complete ref 18, and a detailed description of some parts of our work. This material is available free of charge via the Internet at <http://acsfl@ftp.cas.org>.

(28) Identification of the stationary points associated with the protonation process and the C–C bond formation is in progress.